UV 222 nm emission from KrCl* excimer lamps greatly improves advanced oxidation performance in water treatment

Emma Payne^, Bryan Liu^, Lauren Mullen, Karl G. Linden*

Department of Civil, Environmental, and Architectural Engineering, University of Colorado Boulder, 4001 Discovery Dr., Boulder, CO, 80303, United States

^Emma Payne and Bryan Liu contributed equally as first authors to this work.

*Corresponding author: Karl G. Linden, Tel: (303) 492-4798. Fax: (303) 492-7317. E-mail: karl.linden@colorado.edu

Abstract

KrCl* excimer lamps emitting at 222 nm hold potential for enhancing UV-based advanced oxidation efficiency. Experiments were conducted in both ultrapure water and groundwater comparing low-pressure UV (LPUV) and KrCl* excimer lamps, with two different radical promoters: hydrogen peroxide (H_2O_2) and nitrate (NO_3^-). Compared to conventional LPUV/H_2O_2, the steady state hydroxyl radical (•OH) concentration achieved in the KrCl*/NO_3^- UV/AOP was up to 13.1 times greater while the KrCl*/H_2O_2 process was up to 9.4 times greater in ultrapure water; in groundwater these numbers were 7.3 and 3.7 times greater, respectively, all using a standard single probe compound decay method as a proxy for •OH radical generation. This work identified several research gaps which must be addressed to facilitate adoption of KrCl* for UV/AOP, including development of methods to compare UV/AOPs that utilize different UV radiation sources and radical promoters, a need to develop more information on direct photolysis quantum yields at 222 nm for contaminants of concern, and the impact of the background water matrix constituents on radical promotion or formation of any byproducts, especially in the presence of NO_3^- as a radical promoter.

Keywords: LPUV, KrCl* excimer, hydroxyl radical, hydrogen peroxide, nitrate, advanced oxidation processes (AOPs)

Synopsis: UV advanced oxidation utilizing KrCl* excimer lamp at 222 nm with hydrogen peroxide or nitrate as the radical promoter both performed significantly better at probe compound degradation than conventional UV advanced oxidation with low-pressure UV and hydrogen peroxide.

Graphical Abstract

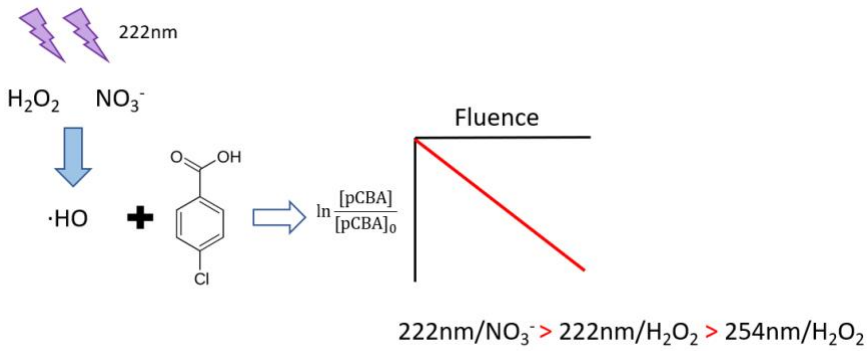

$222nm/NO_3^-$ > $222nm/H_2O_2$ > $254nm/H_2O_2$

Introduction

Ultraviolet (UV)-based advanced oxidation processes (UV/AOPs) are frequently employed in municipal drinking water and water reuse treatment for micropollutant abatement. Common UV/AOPs utilize hydrogen peroxide (H_2O_2) to generate hydroxyl radicals (•OH) under monochromatic low-pressure mercury vapor lamp (LPUV) irradiation at 254 nm or broad spectrum (200-800 nm) irradiation from medium-pressure mercury vapor lamps. This UV/AOP generates hydroxyl radicals via hydrogen peroxide photolysis, which react rapidly (rate constants of 10^7 to 10^{10} $M^{-1}s^{-1}$) and non-selectively with many organic and inorganic contaminants[1,2]. In recent years, the UV-driven production of hydroxyl radicals from species other than hydrogen peroxide has generated interest. AOPs which use chlorine (UV/Cl_2 or UV/NH_2Cl)[3–5] or peroxydisulfate (UV/PDS)[6,7] as the radical promoter are increasingly being studied, and in some cases employed at the pilot or full scale[8,9–11]. Additionally, water matrix constituents such as nitrate or iron can create *de facto* AOPs when exposed to UV light[12–15]. Nitrate absorbs light very strongly at wavelengths below 240 nm to produce hydroxyl and other radicals and has demonstrated potential as a radical promoter in UV/AOP systems which utilize light sources emitting at Far-UVC (200-230 nm) wavelengths[16–18].

Coinciding with the investigation into alternative radical promoters are advancements in UV source technology. Both germicidal UV LEDs and excimer (or exciplex) lamps have emerged in the last decade as potential tools in UV-based water treatment technology[19–21]. Of particular interest here are excimers, which generate deep UV emission when a rare gas or rare gas-halogen dimer returns to ground state from its excited state, with the emission wavelength corresponding to the composition of the dimer[22,23]. KrCl* excimers emit narrow-band UV light at 222 nm and have recently been studied for use in disinfection[20,24,25], greatly enhancing the disinfection of UV-

resistant viruses[26], including for control of SARS-CoV-2[27–29]. KrCl* excimers have advantages over conventional UV sources because they do not contain mercury and the Far-UVC emission at 222 nm is not very harmful to human tissue[30–32], thereby eliminating several hazards typically associated with conventional UV treatment of surfaces, air and water. Few studies have exploited the unique wavelength emission of KrCl* excimers for improving advanced oxidation[33–36].

The goal of this study was to promote radical improvements in AOP treatment through use of 222 nm emitting lamps by comparing •OH generation, as measured by a probe compound, across three UV advanced oxidation systems: conventional LPUV with hydrogen peroxide as the radical promoter (LPUV/H_2O_2), KrCl* excimer with hydrogen peroxide (KrCl*/H_2O_2), and KrCl* excimer with nitrate ($KrCl^*/NO_3^-$). Experiments were conducted both in ultrapure water and a natural groundwater to investigate the rate of •OH production and the impacts of background water constituents on the 222 nm-driven generation of •OH in comparison to conventional LPUV emitting at 254 nm. The opportunities for process optimization by utilizing new UV sources or radical promoters are presented, and the challenges of quantitatively comparing different UV/AOPs are described. Lastly, areas of needed research are proposed to support adoption of 222 nm-driven AOPs.

Materials and Methods

Reagents and test waters

Analytical grade para-chlorobenzoic acid (pCBA) was purchased from Sigma-Aldrich (98%). All stock solutions/chemicals (H_2O_2, pCBA, *tert*-butanol, sodium nitrate) were prepared in ultrapure water (resistance = 18MΩ cm). Two test water matrices were used for UV exposure experiments: ultrapure water and a natural groundwater. Supporting Information (SI) Table S1 presents the

relevant water quality data for both sources. In the LPUV/H_2O_2 and KrCl*/H_2O_2 systems, a peroxide concentration of 10 ppm was used, as this concentration is commonly used in municipal UV/H_2O_2 systems[37–39]. In the KrCl*/NO_3^- system, a concentration of 5 $NO_3^- - N/L$ was used. This concentration has shown to be an optimal point which balances hydroxyl radical generation from nitrate photolysis with scavenging by the build-up of nitrite[40] and is below the US EPA MCL of 10 ppm as N[41] so it is a realistic level of nitrate that may be found in environmental waters.

Exposure Approach

A similar bench-scale UV collimated beam apparatus setup was used for all experiments, based on the design proposed in Bolton and Linden (2003) and depicted in Figure S1. Two UV lamp systems were investigated: 1) LPUV mercury lamp emitting at 254 nm (four 15-watt lamps, #G15T8, USHIO); 2) KrCl* excimer lamp emitting at 222 nm (USHIO, Cypress, CA, USA). Incident UV irradiance (equivalent to fluence rate in a collimated beam system) was measured by a calibrated radiometer (ILT5000 Research Radiometer, International Light Inc.) and detector (Model SED240/W, International Light Inc.).

Analysis

An Agilent 1200 series HPLC equipped with a UV detector and a reverse phase C-18 column (all from Agilent, Santa Clara, CA, USA) was used to analyze pCBA. pCBA was eluted with 10mM phosphoric acid (pH~2.5): methanol (v:v=45:55) using 234 nm for absorbance detection.

TOC was measured using a Sievers M5310C TOC analyzer. Alkalinity was measured using a HACH digital titrator. Nitrate and nitrite were measured using HACH TNT 840 and TNT 839 test vials, respectively, in a HACH DR6000 spectrophotometer.

Fluence Calculations

For this study, the fluence presented was calculated using a "incident fluence rate (E_{Inc})," which is an adaptation from the traditional standard methods presented in Bolton and Linden (2003) (Text S3). The incident fluence rate omits the water factor (WF) from the calculation such that the fluence calculation is based on the total photons entering the water matrix, rather than the average fluence rate delivered to the water volume, which accounts for the background water matrix absorbance and path length. The UV fluence reported in this study is therefore the product of incident fluence rate (E_{Inc}) and exposure time (t), denoted F_{Inc}. All results and figures in this manuscript are presented on the basis of incident fluence (F_{Inc}). Additional details on this calculation, as well as figures with fluence calculated using average fluence rate (E_{avg}), can be found in Text S3 and Figures S3 and S4 in the Supporting Information.

Calculation of scavenging rates and •OH steady state concentration

pCBA was chosen as a probe compound due to its fast reaction with hydroxyl radicals ($k_{\cdot OH/pCBA}$ = 5 x 10^9 M^{-1} s^{-1})[43] and low photolysis rate under both LPUV and MPUV systems [44–49]. The pseudo first-order rate constant (k') of pCBA degradation was determined by plotting the natural logarithm of the ratio of the final (C) and initial (C_0) pCBA concentrations as a function of the incident UV fluence (F_{Inc}), as shown in Eqn. 1.

$$k' = \frac{\ln\left(\frac{[pCBA]}{[pCBA]_0}\right)}{F_{Inc}} \quad (1)$$

The normalized steady-state concentration of hydroxyl radicals was then calculated by solving Eqn. 2 for $[\bullet OH]_{ss}/E_{Inc}$[50]. The steady-state hydroxyl radical concentration was normalized by

incident fluence rate (E_{Inc}) to allow for comparison between different UV/AOPs systems with varying output power.

$$\ln\left(\frac{[\mathrm{pCBA}]}{[\mathrm{pCBA}]_0}\right) = \frac{-k_{\bullet \mathrm{OH,pCBA}}}{E_{\mathrm{Inc}}}[\bullet \mathrm{OH}]_{\mathrm{ss}} \times F_{\mathrm{inc}} \quad (2)$$

Results and Discussion

Direct photolysis and quantum yield determination

While pCBA is widely used as a probe compound to indirectly measure hydroxyl radicals for LPUV and MPUV systems[44–49], no studies to date have investigated the photolysis of pCBA or its utility as a probe compound under 222 nm irradiation. Molar absorptivity of H_2O_2 and pCBA, along with the emission spectrum of LPUV and filtered KrCl* excimer lamp, are shown in Figure S2. At the LPUV emission wavelength of 254 nm, the absorptivity of pCBA was measured as $2704 \pm 145\ \mathrm{M^{-1}cm^{-1}}$ and the quantum yield of pCBA decay was experimentally determined (Text S4) to be $0.022 \pm (2.21 \times 10^{-4})$ mol/Es. These values agree well with values found in literature[2,45]. The absorptivity of pCBA at 222 nm was measured as $8112 \pm 529\ \mathrm{M^{-1}cm^{-1}}$, three times as high as the absorptivity at 254 nm. The quantum yield of pCBA decay at 222 nm was experimentally determined to be $0.047 \pm (6.59 \times 10^{-5})$ mol/Es, twice as high as the quantum yield at 254 nm. At 254 nm the incident fluence-based rate constant of pCBA direct photolysis was $1.02 \times 10^{-4}\mathrm{cm^2mJ^{-1}}$, while at 222 nm it was measured as $5.18 \times 10^{-4}\mathrm{cm^2mJ^{-1}}$. Because the degradation of pCBA under filtered KrCl* excimer is not negligible, the decay rate from direct photolysis must be subtracted to isolate for the degradation rate due to hydroxyl radicals. For consistency, a similar approach was taken with the pCBA decay due to 254 nm exposure.

222 nm irradiation improves radical generation in H_2O_2 -based AOP

In both ultrapure water and groundwater, greater hydroxyl radical production from hydrogen peroxide (10ppm) was achieved in the KrCl* system than in LPUV. In ultrapure water, the overall rate of pCBA degradation was 9.1 times higher in the KrCl*/H_2O_2 system than in LPUV/H_2O_2 (Figure 1a), while it was 3.7 times higher in groundwater (Figure 1b). Direct photolysis partially contributed to the increase in probe compound degradation at 222 nm compared to 254 nm. After subtracting out direct photolysis of pCBA, the indirect photolysis decay of pCBA (a measure of the generation of radicals capable of degrading pCBA) promoted by the KrCl*/H_2O_2 system was 9.4 and 3.7 times higher in ultrapure and groundwater, respectively, compared to LPUV/H_2O_2. The higher molar absorbance of peroxide at 222 nm compared to 254 nm ($99 \pm 1\ M^{-1}cm^{-1}$ vs. $21 \pm 0.2\ M^{-1}cm^{-1}$) leads to significant increases in hydroxyl radical production, creating the possibility for impressive performance improvements in AOP water treatment. Furthermore, the higher direct photolysis at 222 nm in addition to higher radical yield translates to greater treatment efficiency for contaminants which are susceptible either to direct photolysis or reaction with hydroxyl radical, or both.

Under 222 nm, nitrate promotes greater radical generation than H_2O_2

Production of oxidative radicals, as measured by the pCBA degradation minus the component due to direct photolysis, was 1.4 times greater in the KrCl*/NO_3^- system than in the KrCl*/H_2O_2, and 13.1 times greater than in LPUV/H_2O_2, in ultrapure water. Because nitrate does not absorb appreciably at 254 nm, the LPUV/NO_3^- combination is very inefficient for radical generation and was not compared here. Although the rate of pCBA decay was faster with NO_3^- compared to H_2O_2, it was not as significant as would be predicted from the molar absorbance of the relative promoters alone ($2747\ M^{-1}cm^{-1}$ for nitrate and $99\ M^{-1}cm^{-1}$ for peroxide). This is likely due to the production of nitrite, a potent hydroxyl radical scavenger, from the photolysis of nitrate. Nitrite is

produced from nitrate photolysis with a quantum yield of between 9-17% at 254 nm[51]. No nitrite quantum yield data for 222 nm exists in the literature, although the quantum yield of nitrite was found to be twice as high at 228 nm compared to 254 nm[52]. Nitrite reacts with •OH with a rate constant of $1 \times 10^{10}\ M^{-1}s^{-1}$, so scavenging by nitrite can significantly lower the steady state hydroxyl radical concentration in UV/NO_3^- systems[51]. Additionally, nitrite is stringently regulated with a U.S. EPA maximum contaminant level of 1 mg-N/L[41]. However, nitrite may also play an important role in the reaction pathways of radical production from nitrate photolysis, in addition to being a potential photosensitizer itself[51]. While these fundamental photochemical properties of nitrate and nitrite are important to any UV/AOP, their importance is magnified in treatment utilizing 222 nm, as both nitrate and nitrite absorb very strongly at wavelengths below 240 nm. Therefore, the role of nitrite in the KrCl/NO_3^- AOP must be further investigated.

Lastly, UV/NO_3^- systems generate reactive nitrogen species (RNS) such as nitric oxide (•NO), nitrogen dioxide (•NO_2), and peroxynitrite ($ONOO^-$), in addition to •OH[16,53], and their role was not assessed here. By using pCBA as a probe compound, the role of RNS vs. •OH could not be isolated. In the KrCl*/NO_3^- experiments with 100 mM *tert*-butanol (TBA) the rate constant of pCBA decay in the presence of nitrate and TBA was similar to the observed decay rate by pCBA direct photolysis (Figure 1-a2 and 1-a3), indicating either that RNS does not contribute to pCBA degradation or that TBA quenches RNS, which has been observed elsewhere[54]. Therefore, it is possible that RNS were present in the KrCl*/NO_3^- AOP but were not quantified with the pCBA radical probe, although future experiments are needed to determine conclusively whether or not RNS contribute to pCBA degradation. Future work with probe compounds tailored to RNS identification is necessary to definitively determine the significance of RNS to contaminant degradation. Certain contaminants, such as phenolic compounds, are particularly susceptible to

198 reactions with RNS[55]. In such cases, contaminant degradation beyond what would be predicted
199 from the hydroxyl radical concentration alone could be expected, which would further increase the
200 treatment efficiency of KrCl*/NO_3^- compared to KrCl*/H_2O_2. However, in these cases, nitrated or
201 nitrosated transformation products could also be formed. During UV irradiation of nitrate-
202 containing water, nitrogen has been shown to incorporate into NOM to produce nitrogenous
203 disinfection byproducts(N-DBPs)[56,57], resulting in increases in geno- or cytotoxicity[56,58]
204 Furthermore, N-DBPs formed upon subsequent chlorination of UV-irradiated water may have a
205 higher toxicity than regulated DBPs[59,60]. Therefore further study into their formation and risk
206 posed by these potential byproducts is critical. Applications of KrCl*/NO_3^- may be limited to water
207 matrices where the formation potential of nitrogenous byproducts is low.

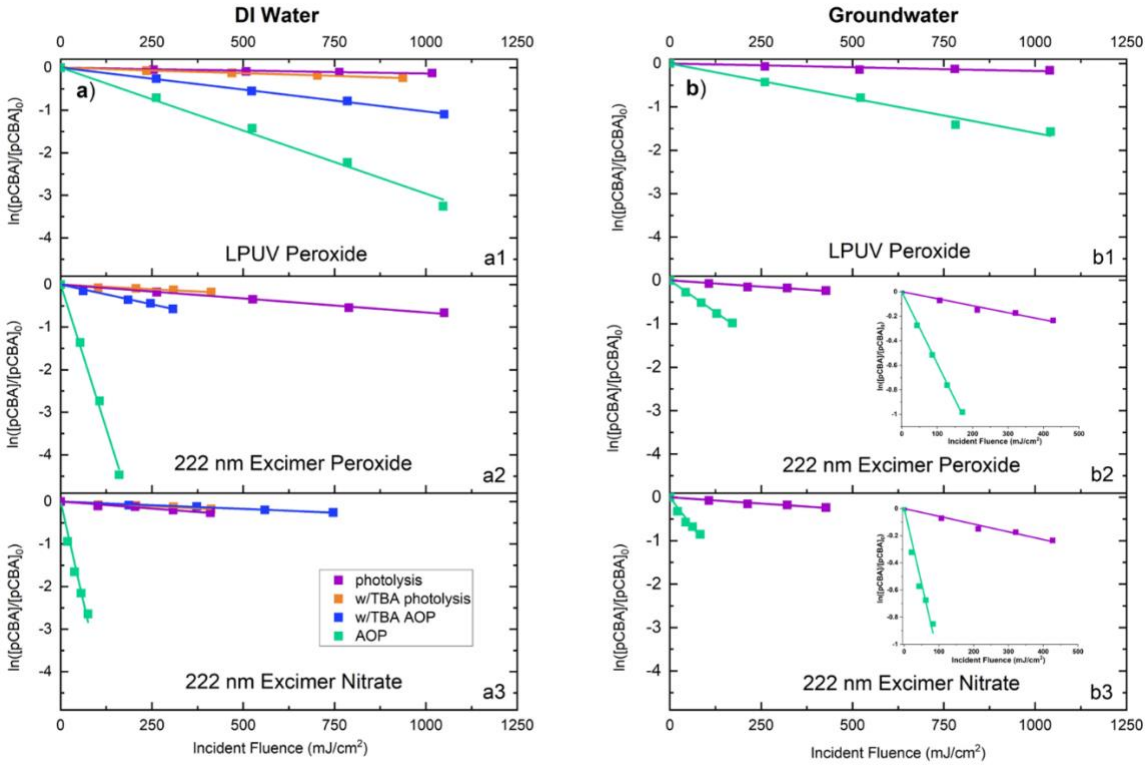

208

209 Figure 1 a) pCBA degradation in three UV/AOPs in ultrapure DI water. b) pCBA degradation in
210 three UV/AOPs in groundwater. The slopes of all linear regressions (i.e., rate of pCBA
211 degradation) are presented in the SI in Tables S3 and S4.

212 ***Impact of water quality on hydroxyl radical yield***

213 Hydroxyl radical production was also investigated in a natural groundwater. pCBA degradation
214 was slower in the groundwater compared to DI in all three UV/AOP systems. In the LPUV/H_2O_2
215 system, the $[OH]_{ss}$, normalized by E_{Inc}, was 49% lower in the groundwater than in the DI water
216 (Figure 2). In the KrCl*/H_2O_2 system $[OH]_{ss}/E_{Inc}$ was 80% lower in the groundwater and in
217 KrCl*/NO_3^- it was 72% lower. The observed decrease in hydroxyl radical steady-state
218 concentration is largely due to scavenging but scavenging alone does not account for the difference
219 between the LPUV/H_2O_2 and KrCl*/H_2O_2 AOPs. These differences could be due to the fact that
220 at 222 nm, the background matrix absorbance is roughly twice the absorbance at 254 nm (Figure

S2b), so the effect of light screening of the water matrix is greater in the excimer systems. In addition to radical scavenging, this could help explain the fact that there is a greater decrease in the hydroxyl radical production in groundwater compared to DI in the excimer-based systems than the LPUV system. Furthermore, because nitrate absorbs more strongly than peroxide, it is less affected by light-screening, explaining why the decrease in $[OH]_{ss}/E_{Inc}$ is slightly less for KrCl*/NO_3^- than KrCl*/H_2O_2, despite scavenging by nitrite in the KrCl*/NO_3^- system. Because the background water matrix absorbs UV light much more strongly at 222 nm than at 254 nm, light screening is an important consideration in KrCl* AOPs. In practical applications with longer light path lengths than the bench study presented here, light screening may significantly hinder the efficiency of a KrCl* AOP. Additionally, the strong light absorption by the water matrix at 222 nm may affect the fluence distribution in a full-scale reactor. As a result, the optimal engineering design for full-scale KrCl* AOPs may be different than for LPUV AOPs and should be investigated. Engineering tools such as computational fluid dynamics (CFD) can be used to determine optimal reactor design to minimize the effect of light screening.

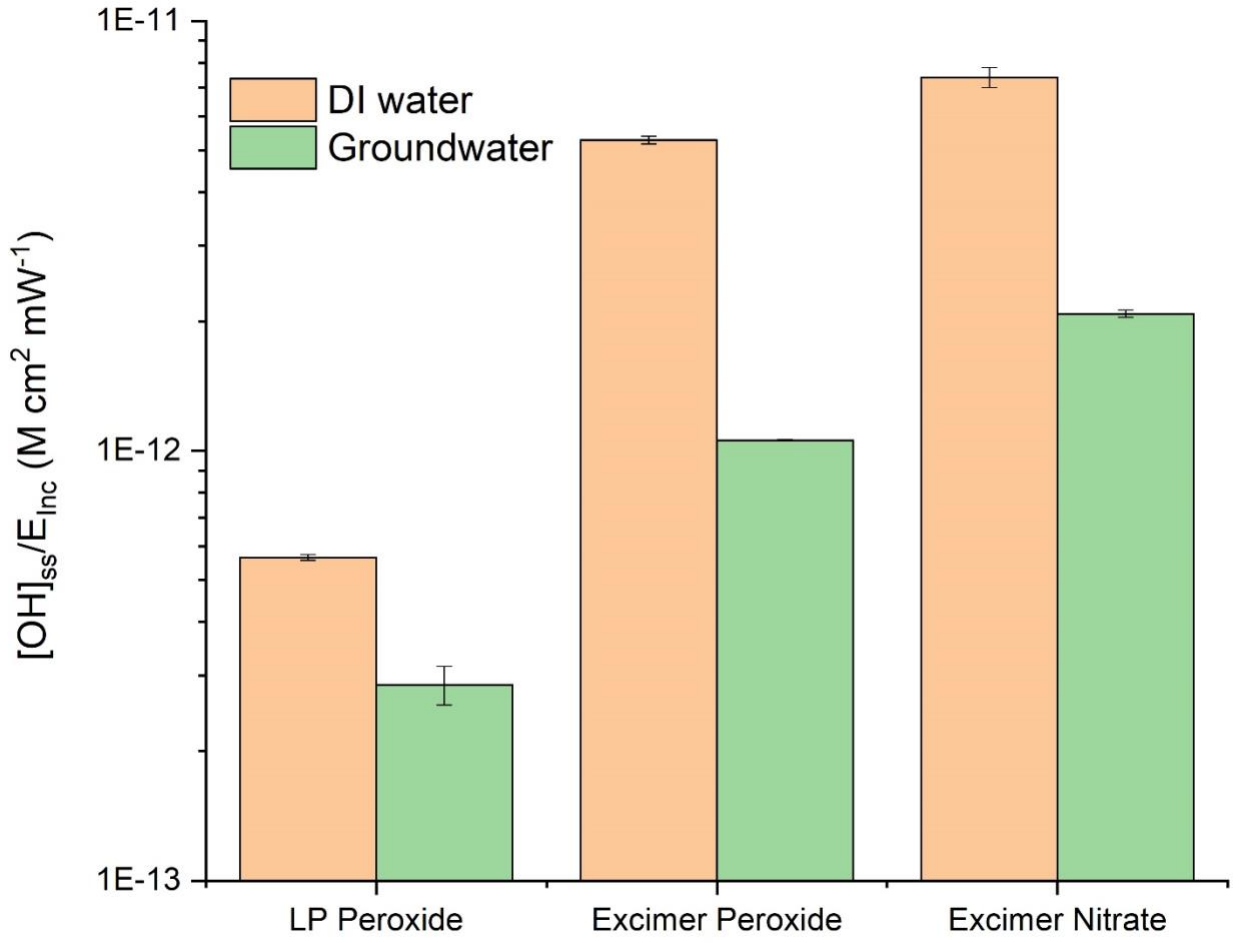

Figure 2. Steady state hydroxyl radical concentration ($[OH]_{ss}$) normalized by incident fluence rate in three UV/AOPs, in both DI and groundwater. Numerical values for each bar are presented in the SI in Tables S3 and S4.

This study was limited to quantifying hydroxyl radical production. However, UV irradiation of natural water containing DOM and alkalinity may generate other radicals such as $^1O_2$[61,62], $^3DOM^*$[62], $CO_3^{\bullet-}$[63], and RNS[64]. $CO_3^{\bullet-}$ forms from the scavenging reaction between CO_3^{2-} and •OH or from the reaction between peroxynitrite, a product of nitrate photolysis[51], and CO_3^{2-} or HCO_3^-[65], and has been demonstrated to significantly contribute to the degradation of certain pesticides[66]. RNS and $^1O_2$/$^3DOM^*$ form from photolysis of nitrate and DOM, respectively, and can also

contribute to contaminant degradation[53,62]. However, the quantum yields or relative abundance of these radicals have not yet been established at 222 nm. Therefore, to better understand the full potential for contaminant degradation in a KrCl* excimer-based UV/AOP, more data on the yield of radical species from background matrix constituents at Far-UVC wavelengths must be investigated.

Challenges and future research for KrCl* excimer UV/AOP

Few data are available in the literature for chemical quantum yields at 222 nm. Future studies should investigate quantum yield of target contaminants. Due to the significantly higher rate of pCBA photolysis observed at 222 nm compared to 254 nm, it is hypothesized that contaminant degradation due to direct photolysis could be significant in KrCl* excimer UV/AOPs, for certain contaminants. Additionally, the radical yield from photolysis of background water matrix constituents at 222 nm should be investigated, as this indirect photolysis could contribute to additional higher-than-expected contaminant degradation.

Background water matrices absorb UV light much greater at 222 nm than 254 nm, therefore, it is important to consider the real-time changes in water quality constituents (i.e., TOC, alkalinity, absorbance, etc.) and the consequent effects (i.e., scavenging, light screening, etc.) throughout the duration of a UV AOP exposure at 222 nm. A dynamic model should be developed to more accurately account for these potentially confounding issues.

Radical promoters absorb differently at 222 nm and 254 nm. In this study, this was illustrated with nitrate, which absorbs over 300x higher at 222 nm than 254 nm. This study utilized a "incident fluence rate" which represents the photons *entering* the water sample, rather than "average fluence rate" which is based on the photons *delivered* to a water volume, corrected for water matrix absorbance and path length. This incident fluence calculation method provides a more equal

comparison between systems with different UV sources, different power outputs, and radical promoters, but adaptable UV models which predict steady-state •OH concentration for varying wavelengths and radical promoters should be investigated. Additionally, methods of comparing the efficiencies of different UV-AOPs on an electrical/chemical cost basis (i.e., the life-cycle costs of the lamp and chemical inputs and electrical energy costs to achieve a certain water quality goal) should be explored.

Associated Content

The Supporting Information is available free of charge at https://pubs.acs.org/XXXXXXX.

SI includes: Water quality and absorbance profiles of test water matrices, UV exposure test set-up, details on adjusted fluence calculation, measured irradiances for each UV exposure, method used for calculating quantum yield, emission plots for KrCl* excimer and LPUV, grapical data on molar absorptivity of peroxide, pCBA, and nitrate, photochemical properties of pCBA, rate constant values for pCBA degradation calculated on both incident and average fluence rate bases for DI and groundwaters, and replotting of the data in Figures 1 and 2 calculated using average fluence.

Acknowledgements

This work was supported by the National Science Foundation-BiNational Science Foundation (NSF-BSF) Award CBET-1931168 to Karl Linden.

Reference

(1) Wols, B. A.; Hofman-Caris, C. H. M.; Harmsen, D. J. H.; Beerendonk, E. F. Degradation of 40 Selected Pharmaceuticals by UV/H2O2. *Water Research* **2013**, *47* (15), 5876–5888. https://doi.org/10.1016/j.watres.2013.07.008.

(2) Wols, B. A.; Hofman-Caris, C. H. M. Review of Photochemical Reaction Constants of Organic Micropollutants Required for UV Advanced Oxidation Processes in Water. *Water Research* **2012**, *46* (9), 2815–2827. https://doi.org/10.1016/j.watres.2012.03.036.

(3) Chuang, Y. H.; Chen, S.; Chinn, C. J.; Mitch, W. A. Comparing the UV/Monochloramine and UV/Free Chlorine Advanced Oxidation Processes (AOPs) to the UV/Hydrogen Peroxide AOP under Scenarios Relevant to Potable Reuse. *Environmental Science and Technology* **2017**, *51* (23), 13859–13868. https://doi.org/10.1021/acs.est.7b03570.

(4) Watts, M. J.; Linden, K. G. Chlorine Photolysis and Subsequent OH Radical Production during UV Treatment of Chlorinated Water. *Water Research* **2007**, *41* (13), 2871–2878. https://doi.org/10.1016/j.watres.2007.03.032.

(5) Guo, K.; Wu, Z.; Chen, C.; Fang, J. UV/Chlorine Process: An Efficient Advanced Oxidation Process with Multiple Radicals and Functions in Water Treatment. *Accounts of Chemical Research* **2022**, *55* (3), 286–297. https://doi.org/10.1021/acs.accounts.1c00269.

(6) Chen, C.; Wu, Z.; Zheng, S.; Wang, L.; Niu, X.; Fang, J. Comparative Study for Interactions of Sulfate Radical and Hydroxyl Radical with Phenol in the Presence of Nitrite. *Environmental Science and Technology* **2020**, *54* (13), 8455–8463. https://doi.org/10.1021/acs.est.0c02377.

(7) Yang, Y.; Pignatello, J. J.; Ma, J.; Mitch, W. A. Comparison of Halide Impacts on the Efficiency of Contaminant Degradation by Sulfate and Hydroxyl Radical-Based Advanced Oxidation Processes (AOPs). *Environmental Science and Technology* **2014**, *48* (4), 2344–2351. https://doi.org/10.1021/es404118q.

(8) Water & Wastewater: Los Angeles Water Reclamation Plant Selects Innovation. *Filtration + Separation* **2015**, *52* (5), 22–23. https://doi.org/10.1016/s0015-1882(15)30219-6.

(9) Kwon, M.; Royce, A.; Gong, Y.; Ishida, K. P.; Stefan, M. I. UV/Chlorine: Vs. UV/H2O2for Water Reuse at Orange County Water District, CA: A Pilot Study. *Environmental Science: Water Research and Technology* **2020**, *6* (9), 2416–2431. https://doi.org/10.1039/d0ew00316f.

(10) Cerreta, G.; Roccamante, M. A.; Oller, I.; Malato, S.; Rizzo, L. Contaminants of Emerging Concern Removal from Real Wastewater by UV/Free Chlorine Process: A Comparison with Solar/Free Chlorine and UV/H2O2 at Pilot Scale. *Chemosphere* **2019**, *236*, 124354. https://doi.org/10.1016/j.chemosphere.2019.124354.

(11) Rott, E.; Kuch, B.; Lange, C.; Richter, P.; Kugele, A.; Minke, R. Removal of Emerging Contaminants and Estrogenic Activity from Wastewater Treatment Plant Effluent with UV/Chlorine and UV/H2O2 Advanced Oxidation Treatment at Pilot Scale. *International Journal of Environmental Research and Public Health* **2018**, *15* (5). https://doi.org/10.3390/ijerph15050935.

(12) Liu, T.; Chen, J.; Li, N.; Xiao, S.; Huang, C.-H.; Zhang, L.; Xu, Y.; Zhang, Y.; Zhou, X. Unexpected Role of Nitrite in Promoting Transformation of Sulfonamide Antibiotics by Peracetic Acid: Reactive Nitrogen Species Contribution and Harmful Disinfection Byproduct Formation Potential. *Environmental Science & Technology* **2021**. https://doi.org/10.1021/acs.est.1c06026.

(13) Zepp, R. G.; Holgne, J.; Bader, H. Nitrate-Induced Photooxidation of Trace Organic Chemicals in Water. *Environmental Science and Technology* **1987**, *21* (5), 443–450. https://doi.org/10.1021/es00159a004.

(14) Keen, O. S.; Love, N. G.; Linden, K. G. The Role of Effluent Nitrate in Trace Organic Chemical Oxidation during UV Disinfection. *Water Research* **2012**, *46* (16), 5224–5234. https://doi.org/10.1016/j.watres.2012.06.052.

(15) Ulliman, S. L.; McKay, G.; Rosario-Ortiz, F. L.; Linden, K. G. Low Levels of Iron Enhance UV/H2O2 Efficiency at Neutral PH. *Water Research* **2018**, *130*, 234–242. https://doi.org/10.1016/j.watres.2017.11.041.

(16) Vinge, S. L.; Shaheen, S. W.; Sharpless, C. M.; Linden, K. G. Nitrate with Benefits: Optimizing Radical Production during UV Water Treatment. *Environmental Science: Water Research and Technology* **2020**, *6* (4), 1163–1175. https://doi.org/10.1039/c9ew01138b.

(17) Sharpless, C. M.; Seibold, D. A.; Linden, K. G. Nitrate Photosensitized Degradation of Atrazine during UV Water Treatment. *Aquatic Sciences* **2003**, *65* (4), 359–366. https://doi.org/10.1007/s00027-003-0674-5.

(18) Luo, C.; Wang, S.; Wu, D.; Cheng, X.; Ren, H. UV/Nitrate Photocatalysis for Degradation of Methylene Blue in Wastewater: Kinetics, Transformation Products, and Toxicity Assessment. *Environmental Technology & Innovation* **2022**, *25*, 102198. https://doi.org/10.1016/j.eti.2021.102198.

(19) Beck, S. E.; Ryu, H.; Boczek, L. A.; Cashdollar, J. L.; Jeanis, K. M.; Rosenblum, J. S.; Lawal, O. R.; Linden, K. G. Evaluating UV-C LED Disinfection Performance and Investigating Potential Dual-Wavelength Synergy. *Water Research* **2017**, *109*, 207–216. https://doi.org/10.1016/j.watres.2016.11.024.

(20) Hull, N. M.; Linden, K. G. Synergy of MS2 Disinfection by Sequential Exposure to Tailored UV Wavelengths. *Water Research* **2018**, *143*, 292–300. https://doi.org/10.1016/j.watres.2018.06.017.

(21) Matafonova, G.; Batoev, V. Recent Advances in Application of UV Light-Emitting Diodes for Degrading Organic Pollutants in Water through Advanced Oxidation Processes: A Review. *Water Research* **2018**, *132*, 177–189. https://doi.org/10.1016/j.watres.2017.12.079.

(22) Kogelschatz, U. Silent Discharges for the Generation of Ultraviolet and Vacuum Ultraviolet Excimer Radiation. *Pure and Applied Chemistry* **1990**, *62* (9), 1667–1674. https://doi.org/10.1351/pac199062091667.

(23) Kogelschatz, U. Excimer Lamps: History, Discharge Physics, and Industrial Applications. *Proceedings of SPIE* **2004**, *5483*, 272–286. https://doi.org/10.1117/12.563006.

(24) Ramsay, I. A.; Niedziela, J. C.; Ogden, I. D. The Synergistic Effect of Excimer and Low-Pressure Mercury Lamps on the Disinfection of Flowing Water. *Journal of Food Protection* **2000**, *63* (11), 1529–1533. https://doi.org/10.4315/0362-028X-63.11.1529.

(25) Tsenter, I.; Garkusheva, N.; Matafonova, G.; Batoev, V. A Novel Water Disinfection Method Based on Dual-Wavelength UV Radiation of KrCl (222 Nm) and XeBr (282 Nm) Excilamps. *Journal of Environmental Chemical Engineering* **2022**, *10* (3), 107537. https://doi.org/10.1016/j.jece.2022.107537.

(26) Beck, S. E.; Rodriguez, R. A.; Linden, K. G.; Hargy, T. M.; Larason, T. C.; Wright, H. B. Wavelength Dependent UV Inactivation and DNA Damage of Adenovirus as Measured by Cell Culture Infectivity and Long Range Quantitative PCR. *Environmental Science and Technology* **2014**, *48* (1), 591–598. https://doi.org/10.1021/es403850b.

(27) Ma, B.; Linden, Y. S.; Gundy, P. M.; Gerba, C. P.; Sobsey, M. D.; Linden, K. G. Inactivation of Coronaviruses and Phage Phi6 from Irradiation across UVC Wavelengths. *Environmental Science and Technology Letters* **2021**, *8* (5), 425–430. https://doi.org/10.1021/acs.estlett.1c00178.

(28) Ma, B.; Gundy, P. M.; Gerba, C. P.; Sobsey, M. D.; Linden, K. G. UV Inactivation of SARS-CoV-2 across the UVC Spectrum: KrCl* Excimer, Mercury-Vapor, and Light-Emitting-Diode (LED) Sources. *Appl Environ Microbiol* **2021**, *87* (22), e0153221. https://doi.org/10.1128/AEM.01532-21.

(29) Kitagawa, H.; Nomura, T.; Nazmul, T.; Omori, K.; Shigemoto, N.; Sakaguchi, T.; Ohge, H. Effectiveness of 222-Nm Ultraviolet Light on Disinfecting SARS-CoV-2 Surface Contamination. *American Journal of Infection Control* **2021**, *49* (3), 299–301. https://doi.org/10.1016/j.ajic.2020.08.022.

(30) Buonanno, M.; Ponnaiya, B.; Welch, D.; Stanislauskas, M.; Randers-Pehrson, G.; Smilenov, L.; Lowy, F. D.; Owens, D. M.; Brenner, D. J. Germicidal Efficacy and Mammalian Skin Safety of 222-Nm UV Light. *Radiation Research* **2017**, *187* (4), 483–491. https://doi.org/10.1667/RR0010CC.1.

(31) Narita, K.; Asano, K.; Morimoto, Y.; Igarashi, T.; Nakane, A. Chronic Irradiation with 222-Nm UVC Light Induces Neither DNA Damage nor Epidermal Lesions in Mouse Skin, Even at High Doses. *PLoS ONE* **2018**, *13* (7), 1–9. https://doi.org/10.1371/journal.pone.0201259.

(32) Buonanno, M.; Welch, D.; Shuryak, I.; Brenner, D. J. Far-UVC Light (222 Nm) Efficiently and Safely Inactivates Airborne Human Coronaviruses. *Scientific Reports* **2020**, *10* (1), 1–8. https://doi.org/10.1038/s41598-020-67211-2.

(33) Gomez, M.; Murcia, M. D.; Gomez, E.; Gomez, J. L.; Dams, R.; Christofi, N. Enhancement of 4-Chlorophenol Photodegradation with KrCl Excimer UV Lamp by Adding Hydrogen Peroxide. *Separation Science and Technology* **2010**, *45* (11), 1603–1609. https://doi.org/10.1080/01496395.2010.487714.

(34) Aseev, D.; Batoeva, A.; Sizykh, M.; Olennikov, D.; Matafonova, G. Degradation of Bisphenol a in an Aqueous Solution by a Photo-Fenton-like Process Using a UV KrCl Excilamp. *International Journal of Environmental Research and Public Health* **2021**, *18* (3), 1–11. https://doi.org/10.3390/ijerph18031152.

(35) Budaev, S. L.; Batoeva, A. A.; Tsybikova, B. A.; Khandarkhaeva, M. S.; Aseev, D. G. Photochemical Degradation of Thiocyanate by Sulfate Radical-Based Advanced Oxidation Process Using UVC KrCl-Excilamp. *Journal of Environmental Chemical Engineering* **2021**, *9* (4), 105584. https://doi.org/10.1016/j.jece.2021.105584.

(36) Murcia, M. D.; Gómez, M.; Gómez, E.; Gómez, J. L.; Christofi, N. Photodegradation of Congo Red Using XeBr, KrCl and Cl2 Barrier Discharge Excilamps: A Kinetics Study. *Desalination* **2011**, *281* (1), 364–371. https://doi.org/10.1016/j.desal.2011.08.011.

(37) Sarathy, S.; Mohseni, M. An Overview of UV-Based Advanced Oxidation Processes for Drinking Water Treatment. *IUVA News* **2006**, *7* (1), 1–12.

(38) Li, D.; Stanford, B.; Dickenson, E.; Khunjar, W. O.; Homme, C. L.; Rosenfeldt, E. J.; Sharp, J. O. Effect of Advanced Oxidation on N-Nitrosodimethylamine (NDMA) Formation and Microbial Ecology during Pilot-Scale Biological Activated Carbon Filtration. *Water Research* **2017**, *113*, 160–170. https://doi.org/10.1016/j.watres.2017.02.004.

(39) Wang, C.; Moore, N.; Bircher, K.; Andrews, S.; Hofmann, R. Full-Scale Comparison of UV/H2O2 and UV/Cl2 Advanced Oxidation: The Degradation of Micropollutant Surrogates and the Formation of Disinfection Byproducts. *Water Research* **2019**, *161*, 448–458. https://doi.org/10.1016/j.watres.2019.06.033.

(40) Lester, Y.; Dabash, A.; Eghbareya, D. Uv Sensitization of Nitrate and Sulfite: A Powerful Tool for Groundwater Remediation. *Environments - MDPI* **2018**, *5* (11), 1–13. https://doi.org/10.3390/environments5110117.

(41) U.S. EPA. National Primary Drinking Water Guidelines. **2009**, No. Epa 816-F-09-004.

(42) Bolton, J. R.; Linden, K. G. Standardization of Methods for Fluence (UV Dose) Determination in Bench-Scale UV Experiments. *Journal of Environmental Engineering* **2003**, *129* (3), 209–215. https://doi.org/10.1061/(ASCE)0733-9372(2003)129:3(209).

(43) Elovitz, M. S.; von Gunten, U. Hydroxyl Radical/Ozone Ratios during Ozonation Processes. I. The R(Ct) Concept. *Ozone: Science and Engineering* **1999**, *21* (3), 239–260. https://doi.org/10.1080/01919519908547239.

(44) Ulliman, S. L.; McKay, G.; Rosario-Ortiz, F. L.; Linden, K. G. Low Levels of Iron Enhance UV/H2O2 Efficiency at Neutral PH. *Water Research* **2018**, *130*, 234–242. https://doi.org/10.1016/j.watres.2017.11.041.

(45) Rosenfeldt, E. J.; Linden, K. G. The ROH,UV Concept to Characterize and the Model UV/H 2O2 Process in Natural Waters. *Environmental Science and Technology* **2007**, *41* (7), 2548–2553. https://doi.org/10.1021/es062353p.

(46) Yuan, F.; Hu, C.; Hu, X.; Qu, J.; Yang, M. Degradation of Selected Pharmaceuticals in Aqueous Solution with UV and UV/H2O2. *Water Research* **2009**, *43* (6), 1766–1774. https://doi.org/10.1016/j.watres.2009.01.008.

(47) Ahn, Y.; Lee, D.; Kwon, M.; Choi, I. hwan; Nam, S. N.; Kang, J. W. Characteristics and Fate of Natural Organic Matter during UV Oxidation Processes. *Chemosphere* **2017**, *184*, 960–968. https://doi.org/10.1016/j.chemosphere.2017.06.079.

448 (48) Watts, M. J.; Linden, K. G. Chlorine Photolysis and Subsequent OH Radical Production
449 during UV Treatment of Chlorinated Water. *Water Research* **2007**, *41* (13), 2871–2878.
450 https://doi.org/10.1016/j.watres.2007.03.032.

451 (49) Shu, Z.; Bolton, J. R.; Belosevic, M.; Gamal El Din, M. Photodegradation of Emerging
452 Micropollutants Using the Medium-Pressure UV/H2O2 Advanced Oxidation Process.
453 *Water Research* **2013**, *47* (8), 2881–2889. https://doi.org/10.1016/j.watres.2013.02.045.

454 (50) Ulliman, S. L.; Miklos, D. B.; Hübner, U.; Drewes, J. E.; Linden, K. G. Improving
455 UV/H2O2 Performance Following Tertiary Treatment of Municipal Wastewater.
456 *Environmental Science: Water Research and Technology* **2018**, *4* (9), 1321–1330.
457 https://doi.org/10.1039/c8ew00233a.

458 (51) Mack, J.; Bolton, J. R. Photochemistry of Nitrite and Nitrate in Aqueous Solution: A
459 Review. *Journal of Photochemistry and Photobiology A: Chemistry* **1999**, *128* (1–3), 1–13.
460 https://doi.org/10.1016/S1010-6030(99)00155-0.

461 (52) Sharpless, C. M.; Linden, K. G. UV Photolysis of Nitrate: Effects of Natural Organic Matter
462 and Dissolved Inorganic Carbon and Implications for UV Water Disinfection.
463 *Environmental Science and Technology* **2001**, *35* (14), 2949–2955.
464 https://doi.org/10.1021/es0020431.

465 (53) Scholes, R. C.; Prasse, C.; Sedlak, D. L. The Role of Reactive Nitrogen Species in
466 Sensitized Photolysis of Wastewater-Derived Trace Organic Contaminants. *Environmental*
467 *Science and Technology* **2019**, *53* (11), 6483–6491.
468 https://doi.org/10.1021/acs.est.9b01386.

469 (54) Wu, Z.; Chen, C.; Zhu, B. Z.; Huang, C. H.; An, T.; Meng, F.; Fang, J. Reactive Nitrogen
470 Species Are Also Involved in the Transformation of Micropollutants by the
471 UV/Monochloramine Process. *Environmental Science and Technology* **2019**, *53* (19),
472 11142–11152. https://doi.org/10.1021/acs.est.9b01212.

473 (55) Castro, G.; Rodríguez, I.; Ramil, M.; Cela, R. Evaluation of Nitrate Effects in the Aqueous
474 Photodegradability of Selected Phenolic Pollutants. *Chemosphere* **2017**, *185*, 127–136.
475 https://doi.org/10.1016/j.chemosphere.2017.07.005.

(56) Liu, X.; Park, M.; Beitel, S. C.; Hoppe-jones, C.; Meng, X.; Snyder, S. A. Formation of Nitrogenous Disinfection Byproducts in MP UV-Based Water Treatments of Natural Organic Matters: The Role of Nitrate. *Water Research* **2021**, 117583. https://doi.org/10.1016/j.watres.2021.117583.

(57) Liu, X.; Chang, F.; Zhang, D.; Ren, M. Influence of Nitrate/Nitrite on the Degradation and Transformation of Triclosan in the UV Based Disinfection. *Chemosphere* **2022**, *298*, 134258. https://doi.org/10.1016/j.chemosphere.2022.134258.

(58) Gong, S.; Ding, C.; Liu, J.; Fu, K.; Pan, Y.; Shi, J.; Deng, H. Degradation of Naproxen by UV-Irradiation in the Presence of Nitrate: Efficiency, Mechanism, Products, and Toxicity Change. *Chemical Engineering Journal* **2022**, *430* (P4), 133016. https://doi.org/10.1016/j.cej.2021.133016.

(59) Muellner, M. G.; Wagner, E. D.; Mccalla, K.; Richardson, S. D.; Woo, Y. T.; Plewa, M. J. Haloacetonitriles vs. Regulated Haloacetic Acids: Are Nitrogen-Containing DBFs More Toxic? *Environmental Science and Technology* **2007**, *41* (2), 645–651. https://doi.org/10.1021/es0617441.

(60) Shah, A. D.; Mitch, W. A. Halonitroalkanes, Halonitriles, Haloamides, and N-Nitrosamines: A Critical Review of Nitrogenous Disinfection Byproduct Formation Pathways. *Environmental Science and Technology* **2012**, *46* (1), 119–131. https://doi.org/10.1021/es203312s.

(61) Dalrymple, R. M.; Carfagno, A. K.; Sharpless, C. M. Correlations between Dissolved Organic Matter Optical Properties and Quantum Yields of Singlet Oxygen and Hydrogen Peroxide. *Environmental Science and Technology* **2010**, *44* (15), 5824–5829. https://doi.org/10.1021/es101005u.

(62) Lester, Y.; Sharpless, C. M.; Mamane, H.; Linden, K. G. Production of Photo-Oxidants by Dissolved Organic Matter during UV Water Treatment. *Environmental Science and Technology* **2013**, *47* (20), 11726–11733. https://doi.org/10.1021/es402879x.

(63) Yan, S.; Liu, Y.; Lian, L.; Li, R.; Ma, J.; Zhou, H.; Song, W. Photochemical Formation of Carbonate Radical and Its Reaction with Dissolved Organic Matters. *Water Research* **2019**, *161*, 288–296. https://doi.org/10.1016/j.watres.2019.06.002.

(64) Mack, J.; Bolton, J. R. Photochemistry of Nitrite and Nitrate in Aqueous Solution: A Review. *Journal of Photochemistry and Photobiology A: Chemistry* **1999**, *128* (1–3), 1–13. https://doi.org/10.1016/S1010-6030(99)00155-0.

(65) Radi, R. Peroxynitrite, a Stealthy Biological Oxidant. *Journal of Biological Chemistry* **2013**, *288* (37), 26464–26472. https://doi.org/10.1074/jbc.R113.472936.

(66) Wu, C.; Linden, K. G. Phototransformation of Selected Organophosphorus Pesticides: Roles of Hydroxyl and Carbonate Radicals. *Water Research* **2010**, *44* (12), 3585–3594. https://doi.org/10.1016/j.watres.2010.04.011.